

# Experimental evidence for a surface distribution of two-level systems in superconducting lithographed microwave resonators

Jiansong Gao, Anastasios Vayonakis, Shewtank Kumar, and Jonas Zmuidzinas

*Division of Physics, Mathematics, and Astronomy,  
California Institute of Technology, Pasadena, CA 91125*

Miguel Daal and Bernard Sadoulet

*Physics Department, University of California at Berkeley, Berkeley, CA 94720*

Benjamin A. Mazin, Peter K. Day, and Henry G. Leduc

*Jet Propulsion Laboratory, California Institute of Technology, Pasadena, CA 91109*

(Dated: March 14, 2008)

## Abstract

We present measurements of the temperature-dependent frequency shift of five niobium superconducting coplanar waveguide microresonators with center strip widths ranging from 3  $\mu\text{m}$  to 50  $\mu\text{m}$ , taken at temperatures in the range 100-800 mK, far below the 9.2 K transition temperature of niobium. These data agree well with the two-level system (TLS) theory. Fits to this theory provide information on the number of TLS that interact with each resonator geometry. The geometrical scaling indicates a surface distribution of TLS, and the data are consistent with a TLS surface layer thickness of order a few nm, as might be expected for a native oxide layer.

Superconducting microresonators have attracted substantial interest for low temperature detector applications due to the possibility of large-scale microwave frequency multiplexing[1, 2, 3, 4, 5, 6, 7, 8, 9]. Such resonators are also being used in quantum computing experiments [10, 11, 12] and for sensing nanomechanical motion[13]. We previously reported that excess frequency noise is universally observed in these resonators regardless of the type of superconductor or substrate being used, and suggested that two-level systems (TLS) in dielectric materials may be responsible for this noise[14]. TLS effects are also observed in superconducting qubits[11]. The TLS hypothesis is strongly supported by the observed temperature dependence of the noise, and also by the observation of temperature-dependent resonance frequency shifts that agree closely with TLS theory[15]. To make further progress, it is essential to constrain the location of the TLS – to determine whether they exist in the bulk substrate or in surface layers, perhaps oxides on the exposed metal or substrate surfaces, or in the interface layers between the metal films and the substrate. In this paper, we provide direct experimental evidence for a surface distribution of TLS.

The unusual physical properties of amorphous materials at low temperatures are consistent with a collection of TLS with a wide range of excitation energies and relaxation rates[16, 17]. The TLS have electric dipole moments that couple to the electric field  $\vec{E}$  of our resonators. For microwave frequencies, and at temperatures  $T$  between 100 mK and 1 K, the resonant interaction dominates over relaxation, which leads to a temperature-dependent variation of the dielectric constant given by[18]

$$\frac{\Delta\epsilon}{\epsilon} = -\frac{2\delta}{\pi} \left[ \text{Re}\Psi \left( \frac{1}{2} + \frac{1}{2\pi i} \frac{\hbar\omega}{kT} \right) - \log \frac{\hbar\omega}{kT} \right] \quad (1)$$

where  $\omega$  is the frequency,  $\Psi$  is the complex digamma function, and  $\delta = \pi P d^2 / 3\epsilon$  represents the TLS-induced dielectric loss tangent at  $T = 0$  for weak non-saturating fields. Here  $P$  and  $d$  are the two-level density of states and dipole moment, as introduced by Phillips[18].

Eq. (1) has been used extensively to derive values of  $Pd^2$  in amorphous materials. If TLS are present in superconducting microresonators, their contribution to the dielectric constant described by Eq. (1) could be observable as a temperature-dependent shift in the resonance frequency. Indeed, it has recently been suggested that the small anomalous low-temperature frequency shifts often observed in superconducting microresonators may be due to TLS effects[19, 20], and in fact excellent fits to the TLS theory can be obtained[15]. Assuming that the TLS are uniformly distributed in a volume  $V_h$  of host material (e.g. a

metal oxide or the bulk substrate) which has a dielectric constant of  $\epsilon_h$ , it can be shown that the fractional resonance frequency shift is given by

$$\frac{\Delta f_r}{f_r} = -\frac{F}{2} \frac{\Delta \epsilon}{\epsilon} \quad (2)$$

where the filling factor  $F$  is given by

$$F = \frac{\int_{V_h} \epsilon_h \vec{E}(\vec{r})^2 d\vec{r}}{\int_V \epsilon \vec{E}(\vec{r})^2 d\vec{r}} = \frac{w_h^e}{w^e}. \quad (3)$$

The factor  $F$  accounts for the fact that the TLS host material volume  $V_h$  may only partially fill the resonator volume  $V$ , giving a reduced effect on the variation of resonance frequency. According to Eq. (3),  $F$  is the ratio of the electric energy  $w_h^e$  stored in the TLS-loaded volume to the total electric energy  $w^e$  stored in the entire resonator.

The key idea of the experiment described in this paper is to measure  $\Delta f_r/f_r$  of coplanar waveguide (CPW) resonators with different geometries in order to obtain values of  $F\delta$  for each geometry. The frequency-multiplexed resonators are all fabricated simultaneously and are integrated onto a single chip, and are measured in a single cooldown. We can therefore safely assume that a single value of the loss tangent  $\delta$  applies for all resonator geometries. This allows the variation of the filling factor  $F$  with geometry to be determined, providing information on the geometrical distribution of the TLS. If TLS are in the bulk substrate with dielectric constant  $\epsilon_r$ , Eq. (3) applied to the CPW field distribution would yield a filling factor  $F \approx \epsilon_r/(\epsilon_r + 1)$  that is independent of the resonator's center strip width  $s_r$ . If instead the TLS are in a surface layer,  $F$  should be dependent on the CPW geometry, scaling roughly as  $1/s_r$ .

We used a device with a 120 nm-thick Nb film deposited on a crystalline sapphire substrate, patterned into five CPW quarter-wavelength resonators with different geometries. Because Nb has a critical temperature  $T_c = 9.2$  K, the effect of superconductivity on the temperature dependence of the resonance frequency is negligible for  $T < 1$  K. As shown in Fig. 1, each resonator is capacitively coupled to a common feedline using a CPW coupler of length  $l_c \cong 200 \mu\text{m}$  and with a common center-strip width of  $s_c = 3 \mu\text{m}$ . The coupler is then widened into the resonator body, with a center-strip width of  $s_r = 3 \mu\text{m}$ ,  $5 \mu\text{m}$ ,  $10 \mu\text{m}$ ,  $20 \mu\text{m}$  or  $50 \mu\text{m}$ , and a length of  $l_r \sim 5$  mm. The ratio between center strip width  $s$  and the gap  $g$  in both the coupler and the resonator body is fixed to 3:2, to maintain a constant impedance of  $Z_0 \approx 50 \Omega$ . The resonance frequencies are  $f_r \sim 6$  GHz, and the coupler is

designed to have a coupling quality factor  $Q_c \sim 50,000$ . The device is cooled in a dilution refrigerator, and its microwave output is amplified using a cryogenic high electron mobility transistor (HEMT) amplifier on the 4 K stage. The complex transmission  $S_{21}$  through the device and HEMT is measured using a vector network analyzer locked to a rubidium frequency standard, and resonance frequencies are obtained by fitting these data[4, 15].

Fig. 2 shows the measured frequency shifts  $\Delta f_r/f_r$  for the five resonators as a function of temperature over the range 100 mK to 800 mK. Although all of the resonators display a common shape for the variation of frequency with temperature, the magnitude of the effect varies strongly with geometry. As shown by the dashed lines in Fig. 2, fits to the TLS model (Eq. 2) generally agree quite well with the data. The nonmonotonic variation of the dielectric constant with temperature is familiar from the TLS literature:  $f_r$  increases ( $\epsilon$  decreases) when  $T > \hbar\omega/2k$ ; a minimum in  $f_r$  (a maximum in  $\epsilon$ ) occurs around  $T = \hbar\omega/2k$ ; at lower temperatures ( $T < 100$  mK), we would expect to see a decrease in  $f_r$  (increase in  $\epsilon$ ) as indicated by the extrapolation of the fit. The largest deviations from the TLS model (about 4%) occur at the lowest temperatures, and are likely due to TLS saturation effects. Indeed, power-dependent frequency shifts of this size are expected theoretically and have also been previously observed experimentally[15]. In this paper, we will ignore these small effects and focus on the geometrical dependence.

With the exception of the 3  $\mu\text{m}$  resonator, the measured values of  $F\delta$  from the fits have to be corrected for the coupler because the coupler's center strip width  $s_c = 3 \mu\text{m}$  differs from that of the resonator,  $s_c \neq s_r$ . In the limit  $l_c \ll l_r$ , it can be shown that the corrected filling factor is given by  $F^* = (F - tF_{3\mu\text{m}})/(1 - t)$ , where  $t = 2l_c/(l_c + l_r)$ . The values of  $F^*\delta$  are listed in Table 1, as well as the ratios relative to the value for 3  $\mu\text{m}$  resonator.

A portion of the CPW inductance per unit length is contributed by the kinetic inductance of the superconductor. The kinetic inductance fraction,  $\alpha$ , depends on CPW geometry and may be determined by measuring resonance frequency shifts at higher temperatures, closer to  $T_c$ [21]. We therefore measured the resonance frequencies at 4.2 K ( $0.46 T_c$ ), allowing the shift  $\Delta f_r(4.2 \text{ K}) = f_r(4.2 \text{ K}) - f_r(100 \text{ mK})$  as well as the kinetic inductance fraction to be calculated for each geometry, as shown in Table 1.

Fig. 3 shows the results for the geometrical scaling of the corrected filling factor  $F^*$  and the kinetic inductance fraction  $\alpha$ , plotted as ratios relative to their respective values for the resonator with a 3  $\mu\text{m}$  wide center strip. The observed strong variation of  $F^*$  with geome-

try immediately rules out a volume TLS distribution, and favors a surface distribution. We investigate this in more detail by comparing the data to two theoretically calculated geometrical factors  $g_m$  and  $g_g$ , which have units of inverse length and are calculated from contour integrals in a cross-sectional plane given by  $g_m = \int_{\text{metal}} \vec{E}^2 dl / V^2$  and  $g_g = \int_{\text{gap}} \vec{E}^2 dl / V^2$ , where  $V$  is the CPW voltage. The first integral is actually a sum of three contour integrals, taken over the surfaces of the three metal conductors, the center strip and the two ground planes. The second contour integral is taken over the two “gaps”, the surface of the exposed substrate in between the conductors. These contours are illustrated in the inset of Fig. 1. The integrals are evaluated numerically using the electric field derived from a numerical conformal mapping solution to the Laplace equation.

According to Eq. (3),  $F^*$  should have the same scaling as  $g_m$  if the TLS are distributed on the metal surface (or at the metal-substrate interface), or as  $g_g$  if the TLS are located on the surface of the exposed substrate. The kinetic inductance of the CPW may also be calculated using a contour integral similar to that of  $g_m$ , except that the integrand is replaced by  $\vec{H}^2$ [21]. Because the magnetic field  $\vec{H}$  is proportional to  $\vec{E}$  for a quasi-TEM mode, we expect the kinetic inductance fraction  $\alpha$  to have the same geometrical scaling as  $g_m$ .

Fig. 3 shows that the four quantities,  $F^*$ ,  $\alpha$ ,  $g_m$  and  $g_g$ , all scale as  $s_r^{-\gamma}$  with  $\gamma = 0.85-0.91$ . The finite thickness of the superconducting film is responsible for the deviations from  $\gamma = 1$ . This is very strong evidence that the TLS have a surface distribution and are not uniformly distributed in the bulk substrate. Our data cannot discriminate between a TLS distribution on the metal surface from a TLS distribution on the exposed substrate surface (the gap), because the corresponding theoretical predictions ( $g_m$  and  $g_g$ ) are very similar and both agree with the data. Future measurements of resonators with various center strip to gap ratios may allow these two TLS distributions to be separated.

The absolute values of  $F^*\delta$  are also of interest. Assuming a typical value of  $\delta \sim 10^{-2}$  for the TLS-loaded material[11], the measured value of  $F^*\delta = 3 \times 10^{-5}$  for the 3  $\mu\text{m}$  resonator yields a filling factor of  $F^* \sim 0.3\%$ . Numerical calculations show that this is consistent with a  $\sim 2$  nm layer of the TLS-loaded material on the metal surface or a  $\sim 3$  nm layer on the gap surface, suggesting that native oxides or adsorbed layers may be the TLS host material.

In summary, the anomalous low-temperature frequency shifts of our superconducting CPW resonators are well explained by a model in which TLS are distributed on the surface of the CPW. The excess frequency noise[2, 14, 15] also displays a strong geometrical

dependence: for a fixed internal power, we find that the noise scales as  $1/s_r^{1.6}$ , consistent with a surface distribution of TLS fluctuators[22]. It therefore seems very likely that the TLS causing the anomalous low-temperature frequency shifts are also responsible for the excess frequency noise. The use of optimized geometries or non-oxidizing materials may therefore offer a route to more sensitive photon detectors. The TLS should also affect the resonator dissipation. At the relatively high power levels used in our experiments, TLS dissipation is strongly saturated[11, 14] and rather high values of the resonator quality factor ( $Q_r > 10^5$ ) are routinely obtained[1]. However, at low enough microwave power, the TLS response should become unsaturated[23] at which point the quality factor should be limited to  $Q_r \sim 1/F\delta$ , or around  $3 \times 10^4$  for the  $3 \mu\text{m}$  resonator described in this paper. This low-power regime is of direct relevance for quantum experiments[10], in which the microwave excitation of the resonator consists of one or a few photons.

We thank John Martinis, Clare Yu and Sunil Golwala for useful discussions. The device was fabricated in the University of California, Berkeley, Microfabrication Laboratory. This work was supported in part by the NASA Science Mission Directorate, JPL, the Gordon and Betty Moore Foundation, and Alex Lidow, a Caltech Trustee.

- 
- [1] B. A. Mazin, P. K. Day, J. Zmuidzinas, and H. G. LeDuc, AIP Conf. Proc. **605**, 309 (2002).
  - [2] P. K. Day, H. G. LeDuc, B. A. Mazin, A. Vayonakis, and J. Zmuidzinas, Nature **425**, 817 (2003).
  - [3] D. R. Schmidt, C. S. Yung, and A. N. Cleland, Appl. Phys. Lett. **83**, 1002 (2003).
  - [4] B. A. Mazin, Ph.D. thesis, Caltech, Pasadena, CA (2004).
  - [5] I. Hahn, B. Bumble, H. Leduc, M. Weilert, and P. Day, AIP Conf. Proc. **850**, 1613 (2006).
  - [6] J. A. B. Mates, G. C. Hilton, K. D. Irwin, L. R. Vale, and K. W. Lehnert, Appl. Phys. Lett. **92**, 023514 (2008).
  - [7] G. Vardoulakis, S. Withington, D. J. Goldie, and D. M. Glowacka, Measurement Science and Technology **19**, 015509 (2008).
  - [8] J. Baselmans, S. J. C. Yates, R. Barends, Y. J. Y. Lankwarden, J. R. Gao, H. Hoevers, and T. M. Klapwijk, J. Low Temp. Phys. **151**, 524 (2008).
  - [9] I. Hahn, P. K. Day, B. Bumble, and H. G. LeDuc, J. Low Temp. Phys. (2008), to be published.
  - [10] A. Wallraff, D. I. Schuster, A. Blais, L. Frunzio, R.-S. Huang, J. Majer, S. Kumar<sup>1</sup>, S. M. Girvin, and R. J. Schoelkopf, Nature **431**, 162 (2004).
  - [11] J. M. Martinis, K. B. Cooper, R. McDermott, M. Steffen, M. Ansmann, K. D. Osborn, K. Cicak, S. Oh, D. P. Pappas, R. W. Simmonds, et al., Physical Review Letters **95**, 210503 (2005).
  - [12] M. A. Sillanpää, J. I. Park, and R. W. Simmonds, Nature **449**, 438 (2007).
  - [13] C. A. Regal, J. D. Teufel, and K. W. Lehnert (2008), arXiv:0801.1827v1.
  - [14] J. Gao, J. Zmuidzinas, B. A. Mazin, H. G. LeDuc, and P. K. Day, Appl. Phys. Lett. **90**, 102507 (2007).
  - [15] S. Kumar, J. Gao, J. Zmuidzinas, B. A. Mazin, H. G. Leduc, and P. K. Day, Appl. Phys. Lett. (2008), #L07-10595, to be published.
  - [16] W. A. Phillips, J. Low Temp. Phys. **7**, 351 (1972).
  - [17] P. W. Anderson, B. I. Halperin, and C. M. Varma, Phil. Mag. **25**, 1 (1972).
  - [18] W. A. Phillips, Rep. Prog. Phys. **50**, 1657 (1987).
  - [19] S. Kumar, P. Day, H. LeDuc, B. Mazin, M. Eckart, J. Gao, and J. Zmuidzinas, APS March Meeting abstract (2006), <http://meetings.aps.org/link/BAPS.2006.MAR.B38.2>.

- [20] R. Barends, J. J. A. Baselmans, J. N. Hovenier, J. R. Gao, S. J. C. Yates, T. M. Klapwijk, and H. F. C. Hoevers, *IEEE Trans. Appl. Supercond* **17**, 263 (2007).
- [21] J. Gao, J. Zmuidzinas, B. A. Mazin, P. K. Day, and H. G. Leduc, *Nucl. Instrum. Methods Phys. Res., Sect. A* **559**, 585 (2006).
- [22] J. Gao, M. Daal, B. A. Mazin, P. K. Day, H. G. Leduc, B. Sadoulet, and J. Zmuidzinas (2008), unpublished.
- [23] A. D. O’Connell, M. Ansmann, R. C. Bialczak, M. Hofheinz, N. Katz, E. Lucero, C. McKenney, M. Neeley, H. Wang, E. M. Weig, et al., *ArXiv e-prints* **802** (2008), 0802.2404.



TABLE 1: Values and ratios

$s_r$	$\Delta f_r(4.2 \text{ K})$	$\frac{\alpha}{\alpha_{3\mu\text{m}}}$	$F^*\delta$	$\frac{F^*}{F_{3\mu\text{m}}^*}$	$\frac{g_{\text{m}}}{g_{\text{m},3\mu\text{m}}}$	$\frac{g_{\text{g}}}{g_{\text{g},3\mu\text{m}}}$
$[\mu\text{m}]$	$[\text{MHz}]$		$\times 10^{-5}$			
3 $\mu\text{m}$	11.1	1	$2.98 \pm 0.12$	1	1	1
5 $\mu\text{m}$	7.41	0.67	$2.00 \pm 0.07$	0.67	0.62	0.64
10 $\mu\text{m}$	4.15	0.37	$1.10 \pm 0.03$	0.37	0.33	0.35
20 $\mu\text{m}$	2.28	0.21	$0.54 \pm 0.03$	0.18	0.17	0.19
50 $\mu\text{m}$	1.02	0.092	$0.24 \pm 0.02$	0.08	0.075	0.086

## FIGURE CAPTIONS

Figure 1

(Color online) An illustration of the CPW coupler and resonator. The inset shows a cross-sectional view of the CPW. The contour of the metal surface and the contour of the exposed surface of the substrate are indicated by the solid line and the dashed line, respectively.

Figure 2

(Color online) Fractional frequency shift  $\Delta f_r/f_r$  as a function of temperature.  $\Delta f_r/f_r$  is calculated using  $\Delta f_r/f_r = [f_r(T) - f_r(800 \text{ mK})]/f_r(800 \text{ mK})$ . The temperature sweep is in steps of 50 mK from 100 mK to 600 mK, and in steps of 100 mK above 600 mK. The markers represent different resonator geometries, as indicated by the values of the center strip width  $s_r$  in the legend. The dashed lines indicate fits to the TLS theory (Eq. 2).

Figure 3

(Color online) The scaling of the measured values of the kinetic inductance  $\alpha$  and TLS filling factor  $F^*$ , as well as the calculated values of the CPW geometrical factors  $g_m$  and  $g_g$ , are shown, as a function of the resonator center strip width  $s_r$ . The top panel shows the ratios of  $\alpha$  ( $r_1$ ),  $F^*$  ( $r_2$ ),  $g_m$  ( $r_3$ ) and  $g_g$  ( $r_4$ ) to their values for the  $3 \mu\text{m}$  resonators. The bottom panel shows these ratios normalized by the kinetic inductance ratio  $r_1$ .

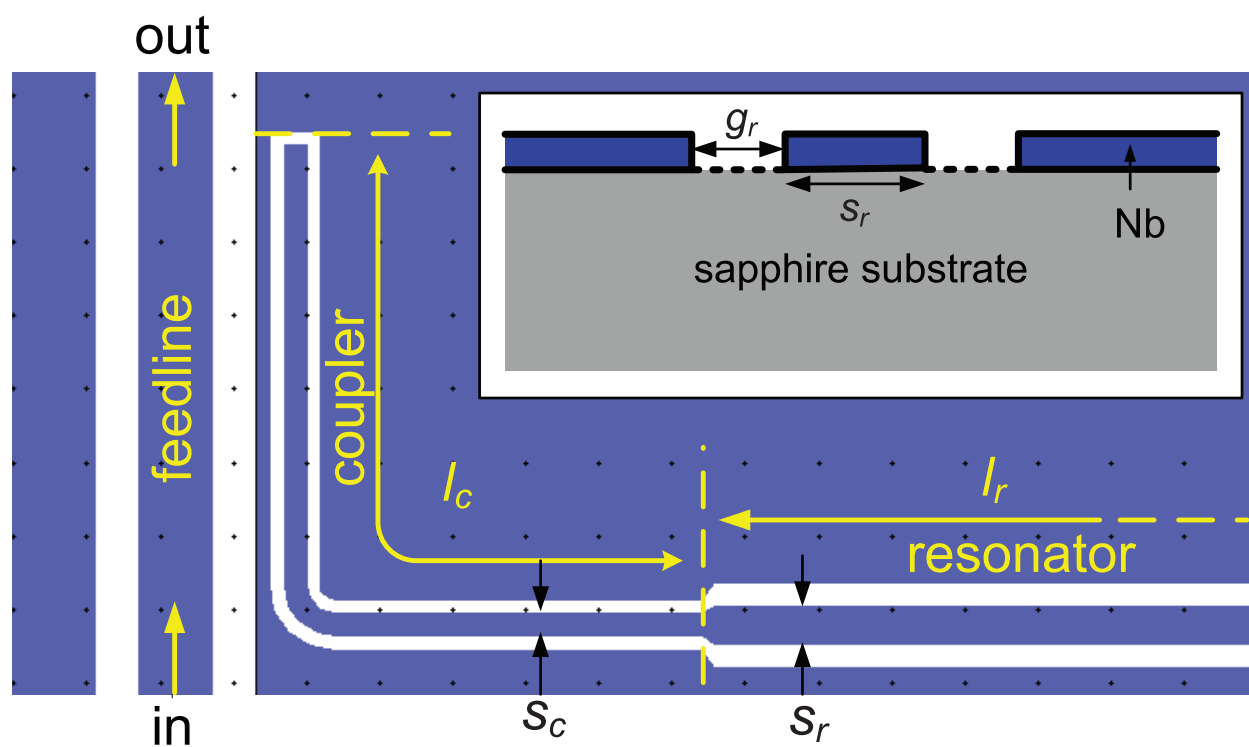


Figure 1

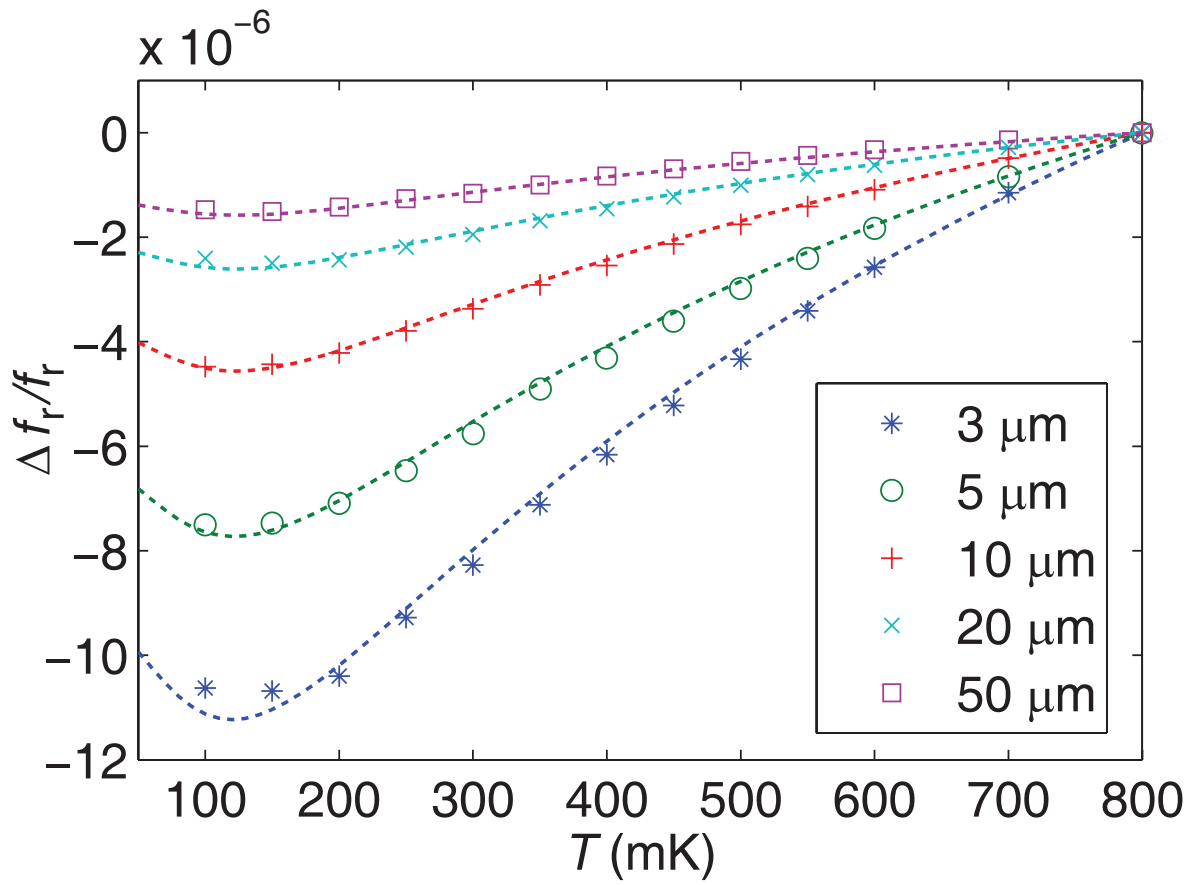


Figure 2

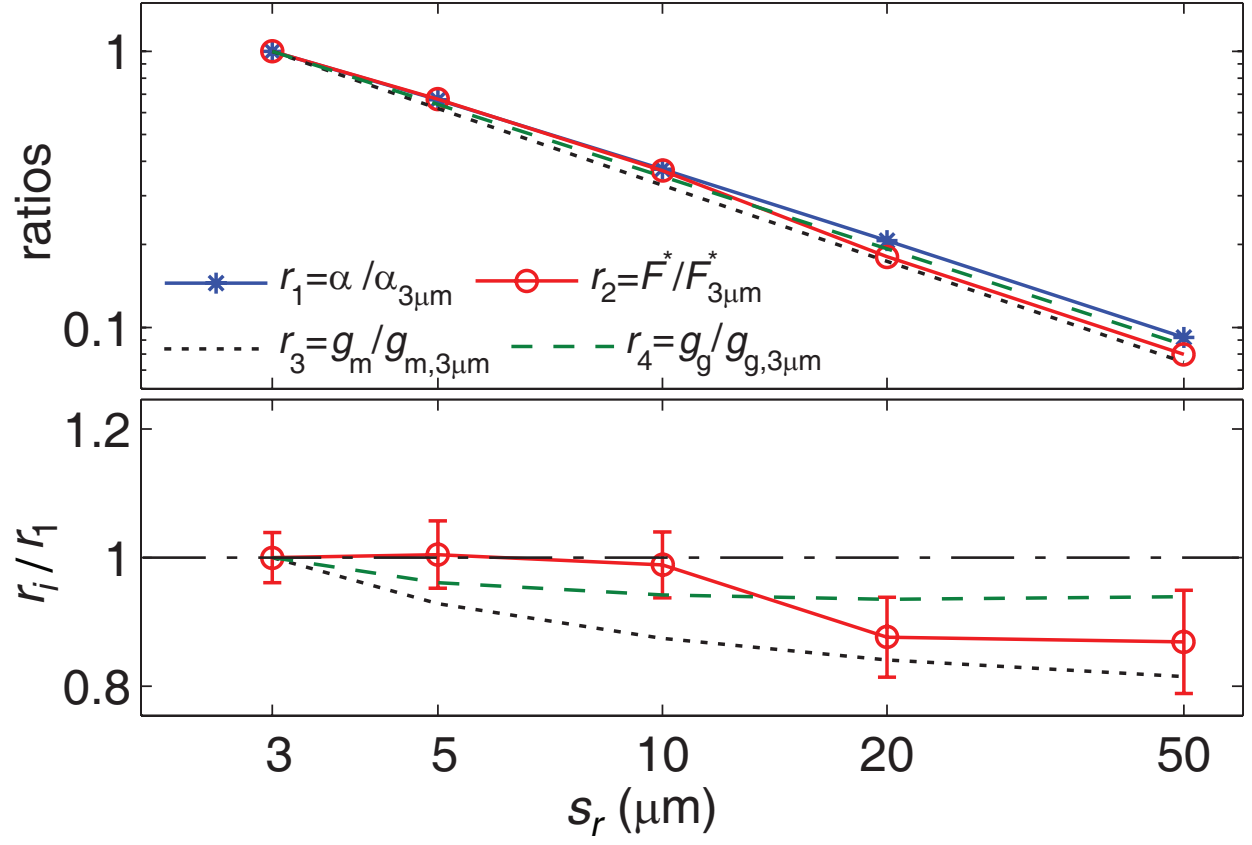


Figure 3